NASA TECHNICAL MEMORANDUM

NASA TM X-3297

POPPET VALVE CONTROL OF THROAT STABILITY BYPASS TO INCREASE STABLE AIRFLOW RANGE OF A MACH 2.5 INLET WITH 60 PERCENT INTERNAL CONTRACTION

Glenn A. Mitchell and Bobby W. Sanders

Lewis Research Center
Cleveland, Ohio 44135

NATIONAL AERONAUTICS AND SPACE ADMINISTRATION • WASHINGTON, D. C. • OCTOBER 1975

1. Report No. NASA TM X-3297	2. Government Accession No.	3. Recipient's Catalog No.
4. Title and Subtitle POPPET VALVE CONTROL OF THROAT STABILITY BYPASS TO INCREASE STABLE AIRFLOW RANGE OF A MACH 2.5 INLET WITH 60 PERCENT INTERNAL CONTRACTION		5. Report Date October 1975
		6. Performing Organization Code
7. Author(s) Glenn A. Mitchell and Bobby W. Sanders		8. Performing Organization Report No. E-8382
		10. Work Unit No. 505-04
9. Performing Organization Name and Address Lewis Research Center National Aeronautics and Space Administration Cleveland, Ohio 44135		11. Contract or Grant No.
		13. Type of Report and Period Covered Technical Memorandum
12. Sponsoring Agency Name and Address National Aeronautics and Space Administration Washington, D.C. 20546		
		14. Sponsoring Agency Code

15. Supplementary Notes

16. Abstract

The throat of a Mach 2.5 inlet with a coldpipe termination was fitted with a stability-bypass system. System variations included several stability-bypass entrance configurations. Poppet valves controlled the bypass airflow. The inlet stable airflow range achieved with each configuration was determined for both steady-state conditions and internal pulse transients. Results are compared with those obtained without a stability-bypass system. Transient results were also obtained for the inlet with a choke point at the diffuser exit and for the inlet with large and small stability-bypass plenum volumes. Poppet valves at the stability-bypass exit provided the inlet with a stable airflow range of 20 percent or greater at all static and transient conditions.

17. Key Words (Suggested by Author(s)) Air intake; Supersonic cruise inlets, Internal compression inlets; Shock wave control; Automatic control valves; Shock stability; Flow stability; Inlet bleed; Throat bypass; Stability bypass	18. Distribution Statement Unclassified - unlimited STAR category 02 (rev.)		
19. Security Classif. (of this report) Unclassified	20. Security Classif. (of this page) Unclassified	21. No. of Pages 47	22. Price* $3.75

POPPET VALVE CONTROL OF THROAT STABILITY BYPASS TO INCREASE

STABLE AIRFLOW RANGE OF A MACH 2.5 INLET WITH

60 PERCENT INTERNAL CONTRACTION

by Glenn A. Mitchell and Bobby W. Sanders

Lewis Research Center

SUMMARY

The throat of a Mach 2.5 mixed-compression inlet having 60 percent internal con-traction was fitted with a stability-bypass system that was designed to provide the inlet with a large stable airflow operating range. Various stability-bypass entrance config-urations were evaluated with a large volume inlet coldpipe to determine the inlet stable airflow range resulting from steady-state conditions and internal transients. The stability-bypass airflow exit was either closed or controlled by poppet valves. Unlike their previous tests, valve oscillation presented their steady-state evaluation. Bench test data indicated that suitable damping eliminated the oscillations. These data were used to predict the steady-state stable range obtainable with suitability damped valves.

Transient stable airflow ranges were also determined for the inlet with a choke point at the compressor face and for the inlet with a large and small stability-bypass plenum volume. Each internal transient was generated by a single sine wave pulse of the overboard-bypass doors. The test was conducted in the Lewis 10- by 10-Foot Supersonic Wind Tunnel at a Mach number of 2.5.

Stability-bypass systems provided the inlet with a large stable airflow range from an inlet operating point having nominal throat airflow removal for boundary-layer con-trol and a total-pressure recovery of about 0.89. It was predicted during steady-state operation that the use of poppet valves would allow inlet airflow to be reduced as much as 24.6 percent without causing unstart, whereas a closed stability-bypass exit (simulating an inlet without a stability-bypass system) allowed a maximum airflow reduction of 7.1 percent. The poppet valves provided the inlet with a relatively large stable airflow range at all the internal transient pulse frequencies (reciprocal of the pulse periods) from from 1 to 40 reciprocal seconds. Airflow stability ranges for the porous stability-bypass entrance configuration with the poppet valves were above 24 percent with the inlet-coldpipe system and above 20 percent with the choke point at the compressor face.

INTRODUCTION

At flight speeds above Mach 2.0 an inlet having a mixture of internal and external compression offers high performance by supplying the engine with airflow at a high pressure level while maintaining low drag. To provide optimum internal performance for this type of inlet, the terminal shock must be kept at the inlet throat. However, mixed-compression inlets suffer from an undesirable airflow characteristic known as unstart. The closer the terminal shock to the throat, the smaller the disturbance that will cause an unstart to occur. This airflow disturbance causes the terminal shock to move forward of the throat where it is unstable, and it is violently expelled ahead of the inlet cowling. This shock expulsion or unstart causes a large rapid reduction in both mass flow and pressure recovery and, thus, a large thrust loss and drag increase. Inlet buzz, compressor stall, and/or combustor blowout may also occur. Obviously, an inlet unstart is extremely undesirable, not only because of the effects on the propulsion system itself, but also on the aerodynamic qualities of the aircraft. If an inlet unstart does occur, large variations of the inlet geometry are required to re-establish initial design operating conditions.

Both external airflow transients such as atmospheric turbulence and internal airflow changes such as a reduction in engine airflow demand can cause the inlet to unstart. It is desirable for the inlet to have a sufficiently large stable margin to absorb such transients without unstarting. For an internal airflow change, the inlet should provide a margin in corrected airflow below the value for optimum performance without incurring unstart. This margin is defined as the stable airflow operating range. Conventional mixed-compression inlets can be designed to have some stable range that is provided by the capacity of the performance bleed systems. Since performance bleed exit areas are generally fixed, this stable range may not be adequate to absorb many of the airflow transients that are encountered by a typical supersonic propulsion system. An increased stable airflow range may be provided by operating supercritically with a resultant loss in performance. Since any loss in performance is reflected directly as a loss in thrust, supercritical operation should be avoided.

To provide the necessary stable airflow range without compromising steady-state performance, the inlet can be designed to replace the throat bleed with a stability-bypass system capable of removing large amounts of airflow when needed. This system prevents unstarts by increasing stability-bypass airflow to compensate for reductions in the diffuser exit airflow demand. References 1 and 2 indicate that large increases in this bypass airflow may be provided without prohibitive amounts of airflow removal during normal operation. These increases in bypass airflow occur when the exit area is controlled to maintain a relatively constant pressure in the bypass plenum. This bypass exit area variation might either be provided by an active control using shock position

sensors or by a passive control such as pressure-activated valves. These valves would open in response to the pressure rise in the stability-bypass plenum caused by the forward moving terminal shock. To be the most effective, the valves should be designed to maintain a nearly constant stability-bypass plenum pressure. Using a Mach 2.5 mixed-compression inlet with 40-percent internal contraction, reference 2 reported that several types of stability-bypass entrance configurations were capable of providing a large stable airflow range if a constant-pressure stability-bypass exit control could be used. When these stability-bypass entrance configurations were used with pressure-activated valves (refs. 3 and 4), the diffuser-exit airflow could be reduced as much as 28 percent from the optimum performance point without causing inlet unstart.

Experimental tests were conducted in the Lewis 10- by 10-Foot Supersonic Wind Tunnel to continue the evaluation of stability-bypass systems. The same types of stability-bypass systems as used in references 3 and 4 were investigated using an axisymmetric, Mach 2.5, mixed-compression inlet having 60 percent of the design supersonic area contraction occurring internally. Stability-bypass airflow was removed from the cowl surface of the inlet throat region through several stability-bypass entrance configurations. These configurations used either a distributed porous surface, distributed "educated" slots, or a forward-slanted slot. The performances of the various stability-bypass configurations are reported in references 5 to 8, wherein choked plug assemblies were used as stability-bypass exit controls and were manually positioned to establish the performance capabilities of each configuration. Stability-bypass entrance configurations of each type were selected from these references to determine their performance with a more sophisticated type of bypass exit control, specifically, pressure-activated poppet valves. Inlet stability limits for these combinations are reported herein for steady-state conditions and for transient internal airflow disturbances. These transient stability limits were determined for an inlet-coldpipe combination. The transients were produced by a single pulse of the diffuser-exit overboard-bypass doors. Pulse periods varied from 1 to 0.025 second; corresponding to sinusoidal frequencies from 1 to 40 hertz. Transient stability limits were also determined for a fixed stability-bypass exit area alternately using a small and large volume stability-bypass plenum. Transient stability limits for the inlet with a choke point at the compressor face were determined for a single stability-bypass entrance configuration. All data were obtained at a free-stream Mach number of 2.5 and a Reynolds number of 3.88×10^6, based on the inlet-cowl-lip diameter.

U.S. customary units were used in the design of the test model and for the recording and computing of experimental data. These units were converted to the International System of Units for presentation in this report.

APPARATUS AND PROCEDURE

Inlet Model

The inlet used in this investigation was a Mach 2.5, axisymmetric, mixed-compression type with 60 percent of the design supersonic area contraction occurring internally. The inlet capture area of 0.1758 square meter sized the inlet to match the airflow requirements of the J85-GE-13 engine at Mach 2.5 and at a free-stream temperature of 390 K. The inlet was attached to a 0.635-meter-diameter cylindrical nacelle in which the J85-GE-13 engine or a coldpipe choked-exit plug assembly could be installed. For this study only the coldpipe was used. Figure 1 shows the test model installed in the wind tunnel test section.

Some of the basic inlet design details are presented in figure 2. Cowl and center-body static-pressure distributions, inlet contours, and diffuser area variations are shown for the inlet design Mach number and spike position. External compression was accomplished with a 12.5° half-angle cone (fig. 3). Translation of this conical center-body provided a varying contraction ratio for off-design operation and inlet restart. At design conditions the cone tip oblique shock passed just ahead of the cowl lip so that approximately 0.25 percent of the capture airflow was spilled over the lip. Internal compression was accomplished with the oblique shock generated by the 0° cowl lip and the two reflected oblique shocks plus isentropic compression between these reflected shocks. As was pointed out in reference 8, the actual oblique shock reflection points were forward of the theoretically predicted points. The geometric throat of the inlet was located at $x/R_c = 3.475$ inlet radii (centerbody surface) where the theoretical average supersonic Mach number was 1.239 with a total-pressure recovery of 0.988. Behind the terminal shock the theoretical recovery was 0.975 at a Mach number of 0.8125.

The subsonic diffuser consisted of an initial throat region, 4 hydraulic radii long with a 1° equivalent conical expansion followed by the main subsonic diffuser. Control of the diffuser-centerbody boundary layer was provided by vortex generators installed at inlet station 98.07 (fig. 3). Details of the vortex generator design are shown in figure 4. The overall inlet length at design, cone tip to compressor face, was 7.72 cowl-lip radii. Internal surface coordinates of the inlet in terms of the cowl-lip radius are presented in table I. A more complete discussion of the inlet design characteristics is presented in reference 9.

In addition to the normally rather long coldpipe at the end of the diffuser, a choke plate could be placed at the diffuser exit (fig. 3). The plate was used during the transient portion of the test to more closely simulate the volume of an inlet-engine combination. The plate reduced the inlet-coldpipe volume from 0.43 to 0.17 cubic meter (table II).

Bleed regions were located in the throat region of the inlet on the cowl and center-body surfaces. As shown in figure 5, the bleed at the forward cowl location was dumped directly overboard. Stability-bypass flow (used to give the inlet a large stable range) was removed through the stability-bypass entrance located on the cowl side of the throat region. Figures 3 and 5 illustrate the ducting of the bypass flow through the cowling to the location of the pressure-activated poppet valves and on to the pipes housing the choked-plug assemblies. Centerbody bleed flow was ducted through hollow support struts to the centerbody bleed pipes (fig. 3). Both the cowl stability-bypass flow and the centerbody bleed flow used two coldpipe choked-plug assemblies each. The remotely actuated plugs that were used to vary these bypass and bleed flows, as well as the main-duct flow, are shown in figure 1(b).

When the choked-plug assemblies were controlling the stability-bypass flow by forming a choked exit at the rear end of the pipes, the poppet valves were in the stability-bypass flow circuit. The valves were in place in the chamber shown in figure 5 but were set in the open position so they would not interfere with the rear choke point. When the poppet valves were used to control the stability-bypass flow, the choke point moved forward so that the effective exit was at the valve location and the bypass choked-plug assemblies were set wide open to prevent choking at the end of the pipes. Poppet valve control of the bypass flow resulted in a small effective bypass plenum volume of about 0.01 to 0.02 cubic meter; coldpipe plug control of the bypass flow resulted in a plenum volume of 0.4 cubic meter, which was almost equal to the main-duct volume of 0.43 cubic meter (table II).

The aft portion of the subsonic diffuser incorporated two remotely controlled bypass systems: a high-response overboard system and a low-speed ejector bypass for engine and nozzle cooling airflow. For steady-state data taking both bypass systems were closed. The high-response overboard system contained six equally spaced doors. These were operated in unison to obtain data on the effect of symmetrical internal transient disturbances to the inlet airflow. The cascades placed at the entrance of the overboard-bypass cavity (fig. 3) minimized a resonant condition in the cavity. A discussion of the resonance that resulted from the open cavity is presented in reference 10.

The photographs and sketches of the test model that have been presented thus far have revealed a bulky external profile. The bulky cowl was used to facilitate the major changes made to the cowl stability bypass and associated ducting during the test, and hence was not representative of flight-type hardware. The sketch in figure 6 shows how a stability-bypass system can be packaged within the low-external-cowl-drag profile essential for supersonic flight.

The three types of stability-bypass entrances that were investigated are shown in figure 7: the distributed porous entrance (fig. 7(a)), the forward-slanted slot entrance (fig. 7(b)), and the distributed educated entrance (fig. 7(c)). The forward cowl bleed was used for a performance bleed and was located forward of each stability-bypass entrance type. As figure 7 shows, the forward cowl bleed was composed of normal holes except when used with the educated configuration. In this instance educated slots were used in place of normal holes. The design of these basic stability-bypass entrances was, for the most part, based on the bleed characteristic information contained in references 11 to 13. These bleed characteristics and the test data (refs. 1 and 9) were used to determine the location and amount of open bypass entrance area for each of the different entrance types.

The distributed porous entrance was extended across the inlet throat region, as shown in figure 7(a), beginning at $x/R_c = 3.282$ inlet radii (just aft of the oblique shock) and ending aft of the throat at $x/R_c = 3.579$ inlet radii. The distributed porous entrance (and the forward cowl bleed region as well) was composed of rows of normal holes. The holes were arranged in a concentrated, staggered pattern, which was intended to prevent flow-induced circumferential variations in the boundary layer. Holes were 0.3175 centimeter in diameter and were drilled normal to the local inlet surface. A nominal porosity of 40 percent was achieved by locating the holes on 0.4763-centimeter centers. Nominal thickness of the metal surfaces in the bleed region or bypass entrance was equal to the hole diameter. The design provided the bypass entrance with the capability of bleeding 27 percent of the inlet capture mass flow.

The same porous design was also incorporated in the forward cowl bleed that was used with the forward-slanted stability-bypass entrance (fig. 7(b)). In concept, a slanted slot entrance is superior to a porous surface entrance in that it provides a higher pressure recovery. Two slot sizes were designed using the slanted slot concept: The larger one was designed to pass 23 percent of the inlet capture airflow and had a slot height of 1.452 centimeter. The smaller slot provided about one half of the bypass entrance area of the larger slot. It was created by adding an insert to the larger slot (as shown in fig. 7(b)). Each slot was flush with the local surface and was slanted away from the surface at a 20° angle. The upstream corner of each slot was sharp, and the downstream lip, before rounding, was located at the inlet geometric throat. A round lip was selected for testing on the basis of the results of a study of effects of lip shape (ref. 2).

The distributed educated bypass entrance (fig. 7(c)) covered about the same region of the inlet throat as did the distributed porous entrance. With the distributed educated entrance, the forward cowl bleed was composed of educated slots rather than normal

holes. The educating technique used herein was an approximation of the ideal rearward slanted hole concept. The rear slant or education theoretically limits the amount of airflow through the holes when the flow over the perforated area is supersonic. With subsonic flow over the perforated area, the airflow through the holes is relatively unaffected by the slant, and a flow coefficient nearly that of a normal hole is predicted. Because of the difficulty of drilling slanted holes in the cowl surface, a number of circumferential slots were used rather than many holes. To educate these slots, the downstream edge was relieved to obtain a 10° angle with the local surface. The slot width was 0.318 centimeter with 1.27 centimeter between adjacent slots. Local porosity resulting from this arrangement was 25 percent and resulted in a stability-bypass entrance capable of theoretically removing 17 percent of the inlet capture mass flow.

The forward centerbody bleed region is shown in figure 8 and was composed of the same concentrated hole pattern that was used for the distributed porous bypass entrance. There were also five rows of holes aft of the inlet throat. Variations from the basic centerbody bleed pattern shown in figure 8 were accomplished by closing selected rows of holes to create a centerbody bleed arrangement that was compatible with the cowl-side stability-bypass entrance. The development of a compatible centerbody bleed arrangement is reported in reference 5. The final arrangement is shown in figure 9; it consisted of three hole rows upstream and three hole rows downstream of the experimental shock impingement point.

The three basic stability-bypass entrance types were used to create the six bypass configurations that were tested during the investigation. Performances of these configurations are reported in references 5 to 8 with the choked plug assemblies controlling the stability-bypass airflow. Four of these configurations are reported herein (fig. 9) with the poppet valves controlling the stability-bypass airflow. Except for the forward-slanted slot, modification of the basic bypass and bleed arrangements shown in figure 7 was accomplished by changing the open areas by filling selected holes and/or slots. Because of these area modifications, the expected mass flow removal capability of the resulting configurations was reduced from that of the completely open area. The distributed porous configuration reported herein could then theoretically remove 18 percent of the inlet capture mass flow. The educated slot configuration could remove 14 percent, the large slot about 11 percent, and the small slot about 6 percent of the inlet capture mass flow. The distributed porous configuration reported herein is configuration NH-3 of reference 5. The educated configuration is the same educated configuration reported in reference 6. Both forward-slanted slots are reported in reference 7.

Pressure-Activated Poppet Valves

Control of the stability-bypass airflow was provided by 16 pressure-activated poppet

valves that were located circumferentially within the inlet cowl. The valves were placed at the exit of the small stability-bypass plenum (figs. 3 and 5). Valves installed in the inlet cowl are shown in figure 10(a), and details of valve mechanical design in figure 10(b). The valve was essentially a floating piston with a trapped volume having a preset internal pressure on one side of the piston. The piston was activated by differential pressure. The internal pressure, inside the valve, was controlled during the test by connection to an external supply. (In a flight situation a suitable internal pressure could be found by a probe on the inlet or airplane and a pressure regulator could be used if necessary. The poppet valve system and its variations are described in a United States patent (ref. 14).) The internal pressure was set to just close the valve during normal inlet operation, that is, with the inlet operating at a high pressure recovery near critical with the terminal shock at the aft edge of the stability-bypass entrance. Under these conditions a perturbation of the inlet terminal shock forward over the stability-bypass entrance would increase the pressure in the bypass plenum above the internal pressure and cause the valve to open and allow bypass flow to occur.

The poppet valve was simply designed with the single intent of demonstrating the feasibility of the concept of constant-pressure control in a stability-bypass plenum. The design allowed the valve to open fully with an increase in pressure on the valve face (stability-bypass total pressure P_{sb}) of only 20 percent. The actual valve performance, as determined on a bench test stand, is shown in figure 10(c) in nondimensional form. The reference pressure $P_{sb, ref}$ was the lowest supply pressure that caused the flow to just choke at the valve attachment bulkhead opening. The reference mass flow $m_{pv, ref}$ was the theoretical flow through the bulkhead opening at this reference pressure (flow coefficient of 1.0). The valve characteristic was indeed quite sensitive to pressure until the flow choked at the valve attachment opening. This choke point was reached with a 25 percent increase in initial operating pressure.

In a flight situation it is probable that many of the perturbations of the inlet shock into the throat region would be quite rapid. It therefore was necessary for the poppet valve to be fast acting in order to absorb such transients. The movable valve head assembly was therefore designed to minimize its weight (fig. 10(b)). For the designed valve head weight of 0.20 kilogram, it was calculated that the valve natural frequency was about 12 hertz at the pressure levels encountered during the test.

Successful steady-state operation of the poppet valves installed in an inlet stability-bypass system is reported in reference 4. However, with some of the stability-bypass entrance configurations of reference 4, the valves were observed to oscillate when partly open during steady-state data taking operations. (With some of the configurations of ref. 4 having steady-state valve oscillations, the valves did not oscillate as long as they were moving in response to a transient, including transients with periods on the order of 20 sec. In a realistic situation it is probable that the valves would never be

open in a steady-state situation but would be moving in response to a transient and thus not oscillate when installed in these configurations.) The instrumentation indicated that the 16 valves oscillated in unison at a frequency of 44 hertz. It was concluded that the valves were acting like second-order dynamic systems, operating well beyond their natural frequency of 12 hertz. In general the oscillations were observed for stability-bypass entrance configurations that provided higher bypass pressure levels with the inlet operating near critical conditions. This effect of pressure on valve oscillation was also observed during the bench test of valve performance. But the addition of a linear potentiometer to measure valve position during the bench test eliminated the oscillations except at very high pressure levels. (Thus ref. 4 concluded that a small amount of properly applied friction might eliminate the oscillation.) Because the throat pressure levels of the inlet of this test were higher than those of reference 4, the valves oscillated when in an open position with each of the stability-bypass entrance configurations. Thus, subcritical steady-state inlet performance with the valves controlling the stability-bypass flow could not be directly determined. Instead, the performance obtainable with suitably damped valves was predicted as follows: The bench test valve performance (e.g., fig. 10(c)) was scaled to the pressure level of each stability-bypass entrance configuration. These data were then plotted on the corresponding bypass performance maps, which were obtained with choked plug assemblies controlling the bypass flow (refs. 5 to 8). The predicted performance is presented in the RESULTS AND DISCUSSION section of this report. Prediction methodology and accuracy are presented in appendix A.

Instrumentation

Inlet total-pressure recovery was determined from the six 10-tube total-pressure rakes that were located at the diffuser exit (fig. 11(a)). Each rake consisted of six equal-area-weighted tubes with additional tubes added at each side of the extreme tubes in positions corresponding to an 18-tube area-weighted rake. The main duct airflow, the centerbody bleed airflow, and the stability-bypass airflow were determined by measurements from the various coldpipe choked-exit plug assemblies shown in figure 1(b). When the stability-bypass was controlled by poppet valves (with the cowl plugs fully open) the stability-bypass mass flow was determined by the method outlined in appendix A.

Bleed flow through the forward cowl bleed region was determined from the measured total and static pressures (fig. 11(b)) and the bleed exit area. Stability-bypass total pressure was obtained from two total-pressure rakes that were located in the bypass plenum at $x/R_c = 4.086$ inlet radii. Pressures from these rakes were averaged

and divided by the free-stream total pressure to obtain the stability-bypass recovery. Centerbody bleed and overboard-bypass total pressures were each measured by a single probe as indicated in figure 11(b). The overboard-bypass total pressure was calibrated to obtain overboard-bypass mass-flow ratio.

Test Procedure

An inlet operating point was selected. From this point, it was desired to determine the effect of the various stability-bypass exit controls on the maximum main-duct airflow reduction possible without causing unstart. The operating point was selected at an inlet recovery of about 0.89, with about 0.02-mass-flow-ratio centerbody bleed and about 0.01 to 0.02 mass-flow ratio through the forward-cowl bleed to minimize the interaction of the cowl reflected shock (fig. 9) with the boundary layer. The overboard bypass was closed for taking steady-state data but still passed 0.01 mass-flow ratio because of leakage. The centerbody bleed flow was set by the choked plugs. For testing with the poppet valves the stability-bypass choked plugs were fully open and the poppet valves were just closed at the inlet operating point by varying the valve internal pressure. Once these items were set, the steady-state stability limits were to be determined by simply closing the main-duct plug from the operating point until unstart occurred. However, because of the valve instability previously discussed, the steady-state stability limits with valve control were determined instead from the bench test data. Stability limits for a closed exit on the small stability-bypass plenum were experimentally determined using the procedure of closing the main-duct plug. The closed exit was obtained by locking the poppet valves closed.

Stability limits were also obtained for transient internal airflow disturbances. The same initial operating point was set as previously described, except that about 60 percent of the main-duct flow was directed through the overboard bypass. The main duct was controlled by the plug or in some cases by the choke plate (fig. 3). The internal transients were generated by pulsing the overboard-bypass doors toward the closed position. A transient consisted of a single sine wave pulse, as shown in figure 12. Each transient command given to the bypass doors is described by the following equations:

$$b = \frac{-B}{2} \left[1 - \cos \frac{2\pi(\text{Time})}{\tau} \right] \quad \text{for} \quad 0 \leq \text{Time} \leq \tau$$

$$b = 0 \quad \text{for} \quad \text{Time} > \tau$$

where B is the amplitude of the commanded door transient, b is the instantaneous amplitude, and τ is the pulse width that was selected. The negative sign simply indicates that the doors were moved toward the closed position. The transient is then described by an equation of harmonic motion where the time span is limited to one period and the frequency is replaced by $1/\tau$. Because the pulse exists for only one period, $1/\tau$ is not a true frequency. However, because people relate more easily to frequency, the results of the transient data are presented in terms of $1/\tau$ and hereinafter called transient pulse frequency.

For each transient pulse width the pulse amplitude was increased until inlet unstart occurred. The amount of bypass-door travel that the inlet would tolerate without unstart was converted to a stability index by means of a bypass-door mass-flow ratio calibration at 90 percent diffuser recovery. The width of the door pulse was varied to obtain the inlet unstart tolerance over a transient pulse frequency range from 1 to 40 reciprocal seconds. At the higher transient pulse frequencies the bypass doors were not capable of producing a pure sine wave at the large amplitudes required at the unstart limit. An example of the door response at 40 reciprocal seconds is shown in figure 12.

Transient stability data were obtained with the stability-bypass flow controlled by either the poppet valves or one of two variations of a closed exit area. One variation was obtained as in the steady-state tests by locking the poppet valves closed. This created the small bypass plenum illustrated in figure 13(a). Plenum volume was 0.01 to 0.02 cubic meter, depending on the bypass configuration used. (See fig. 7 for an example of plenum size variation.) The other closed-exit variation (fig. 13(b)) was obtained by locking the poppet valves open to create a large bypass-plenum volume of approximately 0.4 cubic meter from the throat bypass entrance region back to the closed stability-bypass choked plugs. Whereas the small plenum volume was insignificant in relation to the inlet volume, the large plenum was almost equal to the inlet-coldpipe volume (table II).

RESULTS AND DISCUSSION

Inlet Stability Explanation

The basic types of plots that are used in this report to present the steady-state inlet stability data are explained in this section by using the stylized plots of figure 14. Various performance conditions have been labeled in the figure to aid in the discussion.

The stability-bypass performance is shown in figure 14(a), where the bypass total-pressure recovery is presented as a function of the bypass mass-flow ratio. The series of straight solid lines (A'AB, C'CD, etc.) represent the bypass performance obtainable

with several different fixed exit areas. (Line A'AB represents a closed exit.) Corresponding inlet performance is presented in figure 14(b) by a series of standard diffuser total-pressure-recovery - mass-flow-ratio curves. The diffuser-exit mass-flow ratio, of course, reflects changes in bypass mass-flow ratio and also changes in forward cowl and centerbody bleed mass-flow ratios. (The subcritical stability shown by line AB (fig. 14(b)) is due to the effects of forward cowl and centerbody bleed.) Each solid-line curve represents the performance obtainable with a fixed exit area and corresponds to the solid straight line of identical labeling in figure 14(a). Each of these solid-line curves is generated by reducing the inlet diffuser exit airflow from a supercritical value and causing the inlet terminal shock to move upstream until unstart occurs. By utilizing this mode of operation, locii (dashed curves) of supercritical bypass airflows (A'A C'C E'E G'G) and minimum stable bypass airflows (BDFH) are obtainable. The minimum bypass airflows correspond to supercritical operation. For a given bypass exit area all the supercritical inlet operating points have approximately the same bypass mass-flow and pressure-recovery values. For example, all the inlet operating points between C' and C of figure 14(b) will have the same stability-bypass performance point which is labeled as C'C in figure 14(a). Only when the terminal shock is in the vicinity of the stability-bypass entrance region will shock pressurization occur causing increases in the bypass mass flow and pressure recovery toward their respective maximum values at the minimum stable limit. The bypass and inlet performance maps obtained in the manner just described were initially presented in references 5 to 8 for the inlet reported herein.

To assess inlet stability, it is necessary to look at the change in the diffuser-exit corrected airflow, which is a function of both diffuser-exit mass-flow ratio and total-pressure recovery. Figure 14(c) presents inlet stability, expressed as an airflow index, for the same conditions of figures 14(a) and (b). Values of airflow index (AI) represent the percentage change in corrected airflow between any inlet operating condition and the minimum recorded corrected airflow at point H. Figure 14(c) thus illustrates the amount of stable margin available if the stability-bypass exit area can be varied to guide the inlet operation from any operating condition to an unstart at point H. If a fixed exit area was used to obtain the large stability-bypass airflow available at point H (fig. 14(a)), a prohibitively large amount of bypass airflow would be incurred at supercritical conditions (point G). If the fixed-exit area is reduced to obtain an acceptably low level of supercritical bypass airflow (point A or C), the amount of bypass airflow and consequently the stable margin at the minimum stable condition (point B or D) is also reduced. From the acceptable inlet operating condition of point A (i.e., a high recovery level and a negligible amount of bypass flow), it is apparent that a large stable margin can be had only if the bypass-exit area opens as the inlet proceeds from critical to minimum stable conditions. This type of bypass-exit-area control is provided by

12

poppet valves at the bypass exit. Typical performance for the poppet valves (ref. 4) is shown in figure 14. The poppet valves provide a very large stable margin by allowing the inlet to operate along line AM rather than line AB. This performance is very nearly that which would be provided by an ideal valve having a constant bypass pressure recovery characteristic.

Predicted Steady-State Inlet Stability Limits

The steady-state inlet stability data are presented in figures 15 to 19. A comparison of the inlet stability limits obtained with the four stability-bypass entrance configurations using various bypass exit controls is presented in figure 15. The data from which these stability limits were obtained are presented in figures 16 to 19. These figures present for each bypass entrance configuration the basic data plots as described in figure 14. They show the performance envelope of each configuration as determined in references 5 to 8. They show the performance obtained with a closed stability-bypass exit and the performance predicted for poppet valves at the stability-bypass exit. As explained in the APPARATUS AND PROCEDURE section of this report, the steady-state poppet valve performance was predicted from bench test data (appendix A), rather than experimentally measured, because the valves (when open) oscillated at steady-state conditions when installed in the inlet. The predicted performance represents that expected using a suitably damped poppet valve.

The inlet stability limits shown in figure 15 are presented in terms of stability index. Stability index (SI) is defined as the percentage change in corrected airflow from the inlet operating point to the minimum stable point. The operating point recorded for each bypass entrance configuration is shown by the tailed symbol in figures 16 to 19, and conditions at each operating point are tabulated in figure 15. By referring to appendix B, it can be seen that the equation representing the stability index (SI) is identical to that of the previously discussed airflow index (AI). The difference between the two is as follows: the airflow index (AI) expresses the percentage change in corrected airflow from an operating point to an absolute minimum stable point (point H in fig. 14), and the stability index (SI) represents the percentage change in corrected airflow from an operating point to another minimum stable point reached by an actual bypass exit control (e.g., from point A to point M in fig. 14).

The best potential stability index for each of the tested stability-bypass entrance configurations would be realized by using what is probably the ideal stability-bypass exit control - one having a constant bypass total-pressure recovery characteristic. Such a characteristic was imposed on the experimental bypass performances; the resulting ideal stability index is shown in figure 15 for each bypass entrance configuration. It is

evident that the porous configuration had the largest value of stability index. It obtained an ideal stability index of 26 percent, compared with an index of 12.4 to 17.9 percent for the other configurations.

A large stable range was also predicted when the poppet valves were assumed to control the stability-bypass exit area. Poppet valves at the bypass exit of the distributed porous configuration provided a predicted stability index of 24.6 percent. With the other configurations the stability index predicted by using poppet valves ranged from 9.1 to 17.5 percent. For each bypass entrance configuration the predicted performance was very nearly equal to that obtainable with the ideal constant-recovery bypass exit control; a consequence of the low-pressure-rise characteristic designed into the poppet valve. This characteristic allowed the valve to pass large amounts of stability-bypass flow, as illustrated by the valve performance curve of figure 16(a). The very large "subcritical" stability that the use of the poppet valves gave to the inlet performance is illustrated in figure 16(b).

The variation in stability index predicted for the various stability-bypass entrance configurations using poppet valves (fig. 15) was due to the different performance envelopes of each configuration (parts (a) of figs. 16 to 19). The worse configuration in this regard was the large slot (fig. 17(a)) whose minimum stable line intersected the valve operating line at a low stability-bypass mass-flow ratio. Thus bypass entrance performance, as well as bypass exit control, is important in providing a large stable range.

The amount of stability available to the inlet without a stability-bypass system is represented in figure 15 by the closed stability-bypass exit. With no flow through the stability bypass, some inlet stability was provided by the centerbody and forward cowl bleed systems. These bleed systems represent the so called inlet "performance" bleed that is normally provided to control the throat boundary layer. The performance obtained with these bleed systems is illustrated by the circular data symbols $(\bigcirc)$ appearing in figures 16 to 19. The corresponding data in figure 15 show that inlet performance bleed provided stability indices for the various bypass entrance configurations ranging from 4.5 to 7.1 percent. By controlling the stability bypass with poppet valves, these stability indices could be increased by a factor of 2 to $3\frac{1}{2}$.

With performance bleed alone, the smallest inlet stable range was obtained with the large slot bypass entrance installed in the inlet. The large slot's adverse effect on stability in this instance was due to the effect of the slot on the inlet throat airflow. The slot caused a degradation of the cowl boundary layer and inlet total-pressure recovery which is discussed in reference 8. A similar slot reported in reference 2 installed in another inlet showed no such degradation.

Parts (b) of figures 16 to 19 shows that when poppet valves were assumed to control the stability-bypass exit, the inlet total-pressure recovery increased about 5 percent

14

from the inlet operating point to the minimum stable point. Inasmuch as the stability index is a change in corrected airflow which reflects changes in inlet recovery as well as in mass flow, the increase in inlet total-pressure recovery contributed about a fifth of the stability index obtained with the porous configuration. With a poor configuration like the large slot (fig. 17), where the mass flow change was small, the increase in total-pressure recovery contributed a large share of the stability index: about two thirds. With the stability-bypass exits closed, simulating inlet operation with performance bleed alone, the inlet total-pressure recovery increased about 2 percent from the inlet operating point to the minimum stable point. Among the four bypass entrance configurations, this recovery increase represented from one fifth to one third of the achieved stability index.

Transient Inlet Stability Limits

This section of the report deals with the tolerance of the inlet to internally generated airflow transients. Generation of these transients was accomplished as explained in the section APPARATUS AND PROCEDURE. Transient stability limits of the inlet-coldpipe assembly were obtained for the various stability-bypass exit controls and stability-bypass entrance configurations. These are presented in figure 20 where the transient stability index is plotted as a function of the transient pulse frequency $1/\tau$. These transient data were obtained from inlet operating points that corresponded to the steady-state inlet operating points in figures 16 to 19, except that about 60 percent of the main duct mass flow was directed through the overboard bypass. Points were matched by matching normal shock position and stability-bypass total-pressure recovery. The inlet and stability-bypass total-pressure recoveries that were recorded before obtaining each transient data set are shown in figure 20. Bypass plenum volumes for each configuration are also shown in the figure.

The transient stability limits of the inlet-coldpipe assembly without a stability-bypass system (i.e., the transient stability index available with a normal performance bleed system) is represented in figure 20 by the data having the closed exit with the small-volume stability-bypass plenum (fig. 13). These data show that the transient stability index obtained with a performance bleed system was smaller than that obtained with other stability-bypass exit controls. For all stability-bypass entrance configurations tested, the transient stability index ranged from 3 to 9 percent at a transient pulse frequency of 1 reciprocal second and varied from 16 to 31 percent at a transient pulse frequency of 40 reciprocal seconds. The increase in transient stability index with transient pulse frequency reflects the transient absorption ability of the inlet-coldpipe system volume of 0.43 cubic meter (table II). Except for the large slot configuration, the

transient stability index of all the bypass entrance configurations using performance bleed alone fell within a reasonably narrow, 7 percent, band. The clear deficiency of the transient stability index obtained with the large slot recalls this configuration's steady-state stability-index deficiency and probably results from the same cause.

When the stability-bypass exit was closed in a manner forming a large-volume plenum (fig. 13), the transient stability index obtained with the inlet-coldpipe assembly at a low transient pulse frequency of 1 reciprocal second was nearly the same (within 3 percent) as the index recorded for the closed exit with the small volume (fig. 20). However, with increasing transient pulse frequency, the stability index increased more rapidly when the large volume plenum was installed in place of the small one. In fact, at the highest tested transient pulse frequencies, the transient stability indices of some configurations with the large plenum were so large that they exceeded the transient amplitude limits of the pulsed overboard-bypass doors. The best performance using the closed exit with the large-volume plenum was recorded for the distributed porous configuration. This configuration increased the transient stability index most rapidly with transient pulse frequency and reached the overboard-bypass door limit at a transient pulse frequency of 30 reciprocal seconds with a transient stability index of 54 percent. This is a gain in stability index of 32 percent over the performance obtained when the small bypass plenum (or normal performance bleed system) was used. Although inferior to the porous configuration, the other stability-bypass entrance configurations using the closed exit with the large-volume plenum obtained a stability index in excess of 50 percent at a transient pulse frequency of 40 reciprocal seconds. Their compared performances were somewhat similar to each other in that the stability index curves of all three fell within a stability index band of 5 percent (fig. 20).

The ability of the inlet-coldpipe combination to absorb the large transient pulse amplitudes at the higher internal transient pulse frequencies resulted from the long fill time of the large-volume stability-bypass plenum. This volume of about 0.4 cubic meter, when added to the inlet-coldpipe volume of 0.43 cubic meter, nearly doubled the total system volume. Such a large stability-bypass plenum might be obtained in an actual aircraft by using empty fuel tanks or an internal nacelle volume.

When the poppet valves were installed as a stability-bypass exit control, the resulting transient stability indices of the inlet-coldpipe assembly were larger than those obtained with the other stability-bypass exits at the lower transient pulse frequencies (fig. 20). At a transient pulse frequency of 1 reciprocal second, for example, the transient stability index obtained using the poppet valves varied from 10 to 24 percent among the four stability-bypass entrance configurations. These numbers represent a transient stability index increase of 4 to 15 percent over the index obtained without the valves. The lower performance numbers were those obtained using the inferior large slot configuration.

16

When the transient pulse frequencies were increased, the transient stability indices obtained with the configurations using poppet valve control did not increase as rapidly as those obtained using a closed exit with a large-volume plenum. Although at a transient pulse frequency at 40 reciprocal seconds the transient stability indices obtained using valve control were less than those obtained using the large plenum, they were still quite large. They were (at 40 $\sec^{-1}$) between 49 and 52 percent for all entrance configurations except the large slot which produced a transient stability index of 36 percent. These numbers represent an increase in transient stability index of 19 to 25 percent over the index obtained with performance bleed alone (closed exit with small plenum). In fact, poppet valve exit control produced substantial improvements in transient stability index over the performance bleed values for the complete transient pulse range. Among the four stability-bypass entrance configurations, the minimum transient stability index improvement of between 7 and 20 percent was provided by the large slot configuration. The maximum improvement in transient stability index was recorded for the porous configuration where poppet valve control improved the performance bleed index by between 15 and 29 percent over the transient pulse frequency range. In addition, the porous configuration with poppet valve control provided a transient stability index of over 24 percent at any tested transient pulse frequency.

Placement of a choke plate at the inlet diffuser exit, to more closely simulate inlet-engine volume, reduced the inlet main duct volume from 0.43 to 0.17 cubic meter. The inlet transient stability limits obtained with this reduced inlet volume were determined for the distributed porous configuration and are presented in figure 21. A comparison of this transient stability range with the stability limits obtained using the inlet-coldpipe combination (fig. 20(a)) reveal the expected result: the reduction in system volume reduced the stability range at the higher transient pulse frequencies. The size of the reduction increased as the transient pulse frequency increased. With the closed stability-bypass exit, the inlet transient stability index at a transient pulse frequency of 1 reciprocal second was reduced by only 2 percent by the inlet volume change. But at a transient pulse frequency of 40 reciprocal seconds, the transient stability index obtained using the closed exit with small plenum was reduced from 30 to 15 percent. Similar results were observed when the closed exit with large plenum was used. The inlet volume reduction reduced the transient stability index from 54 to 29 percent at a transient pulse frequency of 30 reciprocal seconds. With poppet valves as a stability-bypass exit control, the inlet transient stability index was reduced about 3 percent by the inlet volume change at low transient pulse frequencies. Again, the inlet volume change caused a greater reduction in transient stability index at the higher transient pulse frequencies. At a transient pulse frequency of 40 reciprocal seconds the inlet volume reduction reduced the transient stability index obtained with the poppet valves from 52 to 23 percent. In spite of such reductions, the inlet with the choke plate and the

poppet valves as a stability-bypass exit control provided a transient stability index of 20 percent or greater over the transient pulse frequency range from 1 to 40 reciprocal seconds.

The stable airflow operating range provided by the stability-bypass systems reported herein may possibly be improved by combining the performance of these systems with the performance of other inlet control hardware. To achieve stability with an inlet-engine combination, the inlet airflow could be matched to that demanded by the engine by a sophisticated closed-loop high-response overboard-bypass system. However, if a stability-bypass with a large volume plenum and closed exit were used in combination with an overboard bypass, a large stable airflow range could be achieved over the complete transient pulse frequency range with a moderate - rather than high-response overboard bypass. Since the poppet valves provide a large transient stability capability at all transient pulse frequencies, an inlet using the valves would need only a relatively slow, unsophisticated, overboard-bypass system to match inlet-engine airflow requirements. If necessary, the transient stability provided by using the poppet valves could be increased at the higher transient pulse frequencies by placing the valves at the exit of a large bypass plenum to utilize the very large high transient pulse frequency stability afforded by the large volume.

SUMMARY OF RESULTS

A stability-bypass system was installed on the cowl side of the throat of a Mach 2.5 mixed-compression inlet having 60 percent internal contraction. Airflow entered the stability-bypass system through either a distributed porous surface, distributed educated slots, or a forward-slanted slot. The stability-bypass airflow exit was either closed or controlled by poppet valves. Unlike their action in some previous tests, the installed poppet valves oscillated when open and prevented steady-state stable range measurements. Bench tests of the poppet valves indicated that suitable damping would eliminate the oscillations. Therefore, the steady-state stability limits obtainable with a suitably damped valve were predicted using bench test valve data (appendix A). These data are compared with the experimentally obtained stability limits with a closed stability-bypass exit to simulate the inlet without a stability-bypass system. Transient stability limits were experimentally determined for both the inlet-coldpipe assembly and the inlet with a choke point at the diffuser exit, with each of these main duct volume variations having the stability-bypass exit controlled by the poppet valves or closed with alternately small and large volume stability-bypass plenums. The test was conducted in the Lewis 10- by 10-Foot Supersonic Wind Tunnel at a Mach number of 2.5 with the following results:

18

1. With the inlet operating at a total-pressure recovery of about 0.89, stability-bypass systems with valve-controlled exits could provide the inlet with a large stable airflow operating range. During steady-state operation, the stability-bypass performance predicted for poppet valve exit control would allow the inlet airflow to be reduced by as much as 24.6 percent without causing unstart; whereas, a closed bypass exit (simulating no bypass system) allowed a maximum of 7.1 percent.

2. The poppet valves provided the inlet with a relatively large stable airflow range over the tested transient pulse frequency range from 1 to 40 reciprocal seconds. Airflow stability ranges were above 24 percent for the porous stability-bypass entrance configuration using poppet valve control and the large volume inlet-coldpipe combination.

3. A closed stability-bypass exit having a large volume plenum provided the inlet-coldpipe combination with the largest transient stable airflow operating range at the higher transient pulse frequencies (a transient stability of 54 percent of engine airflow at a pulse frequency of 30 sec^{-1} for the porous configuration and over 50 percent at 40 sec^{-1} for all other stability-bypass entrance configurations). At a transient pulse frequency of 1 reciprocal second the large volume plenum achieved little improvement over the transient inlet stability obtained with the small volume plenum.

4. With the inlet volume reduced by a choke point at the diffuser exit, the transient stable margin obtained at the higher transient pulse frequencies was smaller than that obtained with the larger volume inlet-coldpipe combination. Despite these reductions, the porous stability-bypass entrance configuration with poppet valves controlling the bypass exit obtained a transient stable margin above 20 percent over the transient pulse frequency range of 1 to 40 reciprocal seconds.

Lewis Research Center,
    National Aeronautics and Space Administration,
        Cleveland, Ohio, July 9, 1975,
            505-04.

APPENDIX A

PREDICTED STEADY-STATE INLET STABILITY PERFORMANCE

The stability of an inlet with a stability-bypass system is dependent on the performance map of the particular stability-bypass entrance configuration and the pressure recovery mass-flow ratio characteristic of the bypass exit control (fig. 22(a)). Although inlet stability can be determined by experimental testing with each stability-bypass entrance and exit control, the stability performance should be predictable if the performance map of the stability-bypass entrance configuration is known and the pressure recovery mass-flow ratio characteristic of the exit control can be determined from a bench test.

The method of predicting inlet stability is outlined herein using the bench test data of the poppet valves described in figure 10(c) and the performance map of a stability-bypass system installed in another inlet (distributed-porous configuration II of ref. 4, fig. 22(a)). This inlet used a bicone centerbody, rather than the single cone design of the inlet of this report, and differed in throat Mach number and amount of internal compression.

The bench test performance of the poppet valve was scaled to the stability-bypass total-pressure level of the distributed-porous configuration II obtained with the inlet functioning at the selected operating point. (The valve operating pressure of 0.8 $P_{sb}/P_{sb,ref}$ in fig. 10(c) was equated to the pressure level of the tailed symbol in fig. 22(a).) The scaled valve performance data were plotted on the stability-bypass performance map by placing the valve closed point at the inlet operating point (fig. 22(a)) and terminating the generated curve at the inlet minimum stable line. The resulting curve predicts the poppet valve performance when installed at the exit of the distributed-porous configuration II in the inlet of reference 4.

The inlet performance curve predicted for the poppet valves (fig. 22(b)) was obtained as follows. Values of stability-bypass mass-flow ratio were picked from the bypass performance map at points where the predicted poppet valve curve crossed lines of constant bypass-exit area and the minimum stable line. Another performance map (not shown), in which inlet total-pressure recovery was plotted against stability-bypass mass-flow ratio, was then used. The picked values of stability-bypass mass-flow ratio were plotted on this map on their corresponding constant bypass-exit area lines and minimum stable line. This procedure determined the inlet total-pressure recovery at each of the picked values. Each total-pressure recovery was plotted on its corresponding line on the inlet performance map (fig. 22(b)) to form the predicted inlet performance curve. Similarly, values of stability-bypass total-pressure recovery were picked from the bypass performance map and plotted on their corresponding lines in figure 22(c)

20

to predict the airflow index curve.

Figure 22 also presents experimental performance data obtained with the poppet valves installed in the inlet of reference 4. The predicted poppet valve performance agrees very well with the experimental poppet valve performance. The predicted inlet recovery curve is up to 1 percent lower than the experimental curve but most of this difference was due to insufficient performance map data. This necessitated the use of straight line segments in the constant bypass exit curves which lowered the picked values of inlet total pressure.

Inlet stability is presented in reference 4 in terms of a stability index which is defined as the percentage change in corrected airflow from the inlet operating point to the minimum stable point determined by the bypass exit control. Reference 4 reports that the stability index achieved with distributed-porous configuration II using poppet valves was 28 percent. The stability index obtained using the predicted valve performance was 28.3 percent.

APPENDIX B

SYMBOLS

A   flow area, m^2

AI   airflow index in percent, $AI = 100 \left\{ 1 - \left[(W_{corr})_{min\ s} / (W_{corr})_{op} \right]_5 \right\}$

A_c cowl-lip capture area, $0.1758\ m^2$

C   converging vortex generator pair

D   diverging vortex generator pair

d   distance from local surface, cm

H   annulus height, cm

M   Mach number

m   mass flow, kg/sec

P   total pressure, N/m^2

p   static pressure, N/m^2

R_c inlet-cowl-lip radius, 23.66 cm

r   radius, cm

SI   stability index in percent, $SI = 100 \left\{ 1 - \left[(W_{corr})_{min\ s} / (W_{corr})_{op} \right]_5 \right\}$

W_{corr} corrected airflow, kg/sec

x   axial distance from cone tip, cm

θ_l cowl-lip position parameter, $\tan^{-1}\left[1/(x/R_c) \right]$

τ transient pulse width, sec

φ circumferential position, deg

subscripts:

av   average

cb   centerbody bleed

e   exhaust

fc   forward cowl bleed

min s   minimum stable inlet operating point

op   inlet operating point

pv	poppet valve
pvi	poppet valve, internal
ref	reference
sb	stability bypass
x	value at distance x
0	free stream
5	diffuser exit

REFERENCES

1. Sanders, Bobby W.; and Cubbison, Robert W.: Effect of Bleed-System Back Pressure and Porous Area on the Performance of an Axisymmetric Mixed-Compression Inlet at Mach 2.50. NASA TM X-1710, 1968.

2. Sanders, Bobby W.; and Mitchell, Glenn A.: Throat-Bypass Bleed Systems for Increasing the Stable Airflow Range of a Mach 2.50 Axisymmetric Inlet with 40-Percent Internal Contraction. NASA TM X-2779, 1973.

3. Sanders, Bobby W.; and Mitchell, Glenn A.: Increasing the Stable Operating Range of a Mach 2.5 Inlet. AIAA Paper 70-686, June 1970.

4. Mitchell, Glenn A.; and Sanders, Bobby W.: Pressure-Activated Stability-Bypass-Control Valves to Increase the Stable Airflow Range of a Mach 2.5 Inlet with 40-Percent Internal Contraction. NASA TM X-2972, 1974.

5. Shaw, Robert J.; Mitchell, Glenn A.; and Sanders, Bobby W.: Distributed Porous Throat Stability Bypass to Increase the Stable Airflow Range of a Mach 2.5 Inlet with 60-Percent Internal Contraction. NASA TM X-2974, 1974.

6. Shaw, Robert J.; Mitchell, Glenn A.; and Sanders, Bobby W.: Distributed Educated Throat Stability Bypass to Increase the Stable Airflow Range of a Mach 2.5 Inlet with 60-Percent Internal Contraction. NASA TM X-2975, 1974.

7. Shaw, Robert J.; Mitchell, Glenn A.; and Sanders, Bobby W.: Forward-Slanted Slot Throat Stability Bypass to Increase the Stable Airflow Range of a Mach 2.5 Inlet with 60-Percent Internal Contraction. NASA TM X-2973, 1974.

8. Mitchell, Glenn A.; Sanders, Bobby W.; and Shaw, Robert J.: Throat Stability-Bypass Systems to Increase the Stable Airflow Range of a Mach 2.5 Inlet with 60-Percent Internal Contraction. NASA TM X-2976, 1974.

9. Cubbison, Robert W.; Meleason, Edward T.; and Johnson, David F.: Effect of Porous Bleed in a High-Performance Axisymmetric, Mixed-Compression Inlet at Mach 2.50. NASA TM X-1692, 1968.

10. Coltrin, Robert E.; and Calogeras, James E.: Supersonic Wind Tunnel Investigation of Inlet-Engine Compatibility. AIAA Paper 69-487, June 1969.

11. McLafferty, George M.: A Stepwise Method for Designing Perforated Supersonic Diffusers. Rep. R-12133-5, United Aircraft Corp., 1949.

12. McLafferty, George M.: A Study of Perforated Configurations for Supersonic Diffusers. Rep. R-53372-7, United Aircraft Corp., 1950.

13. McLafferty, George M.; and Ranard, E.: Pressure Losses and Flow Coefficients of Slanted Perforations Discharging From Within a Simulated Supersonic Inlet. Rep. R-0920-1, United Aircraft Corp., 1958.

14. Mitchell, Glenn A.; and Sanders, Bobby W.: Airflow Control System for Supersonic Inlets. U.S. Patent 3,799,475, Mar. 1974.

TABLE I. - INLET INTERNAL SURFACE COORDINATES

(a) Centerbody

Axial distance from cowl lip, x/R_c, inlet radii	Radial distance, r/R_c, inlet radii	Axial distance from cowl lip, x/R_c, inlet radii	Radial distance, r/R_c, inlet radii
0	0	4.402	0.609
12.5° Half angle conical section		4.563	.588
2.885	.640	4.724	.566
2.924	.649	5.161	.498
2.952	.655	5.261	.481
3.017	.667	5.361	.462
3.081	.678	5.461	.444
3.124	.684	5.561	.418
3.178	.691	5.661	.409
3.221	.696	5.761	.396
3.237	.700	5.861	.373
3.306	.703	5.961	.357
3.349	.705	6.061	.341
3.403	.707	6.161	.327
3.435	.708	6.261	.313
3.446	↓	6.361	.299
3.457		6.461	.285
3.468		6.561	.272
3.478	.707	6.661	.260
3.489	.706	6.761	.250
3.543	.702	6.861	.243
3.596	.697	6.961	.240
3.650	.691	7.061	.239
3.865	.670	Cylinder	
3.972	.660		
4.079	.649	7.946	0.239
4.120	.644		
4.187	.636		
4.240	.635		
4.294	.623		

TABLE I. - Concluded.

(b) Cowl

Axial distance from cowl lip, x/R_c, inlet radii	Radial distance, r/R_c, inlet radii	Axial distance from cowl lip, x/R_c, inlet radii	Radial distance, r/R_c, inlet radii	Axial distance from cowl lip, x/R_c, inlet radii	Radial distance, r/R_c, inlet radii
2.009	1.000	3.446	0.952	5.461	0.913
2.156	↓	3.457	.951	5.561	.916
2.297		3.468	.951	5.661	.917
2.383		3.478	.950	5.761	.918
2.469		3.489	.949	Cylinder	
2.491		3.543	.945	6.235	0.918
2.512		3.596	.942	Bypass gap	
2.566	.999	3.650	.939	6.845	0.887
2.630	.997	3.756	.932	6.861	.887
2.695	.995	3.863	.925	6.961	.885
2.738	.994	3.970	.919	7.061	.882
2.811	.992	4.088	.913	7.161	.879
2.860	.989	4.093	.913	7.261	.873
2.885	.988	4.189	.909	7.361	.868
2.924	.986	4.267	.906	7.461	.864
2.952	.985	4.277	.905	7.561	.863
3.017	.981	4.384	.903	7.661	.862
3.081	.979	4.545	.902	Cylinder	
3.124	.976	4.706	.902	7.946	0.862
3.178	.972	4.868	.903		
3.221	.971	5.029	.904		
3.237	.966	5.093	.904		
3.306	.963	5.161	.905		
3.350	.960	5.261	.907		
3.403	.955	5.361	.910		
3.435	.953				

TABLE II. - INLET VOLUMES

Configuration	Main-duct volume, m^3	Stability-bypass plenum volume, m^3
Inlet-coldpipe combination with -		
Small stability-bypass plenum	0.43	~ 0.01 to 0.02
Large stability-bypass plenum	.43	~ 0.4
Inlet with choke plate and -		
Small stability-bypass plenum	.17	~ 0.01 to 0.02
Large stability-bypass plenum	.17	~ 0.4

(a) Front view.

Choked plug assemblies
for centerbody bleed flow

Centerbody bleed
pipe (1 of 2)

Choked plug
assembly for
diffuser-exit flow

Stability-bypass
pipe (1 of 2)

Choked plug
assemblies for
stability-bypass flow

C-70-3482

C-69-3872
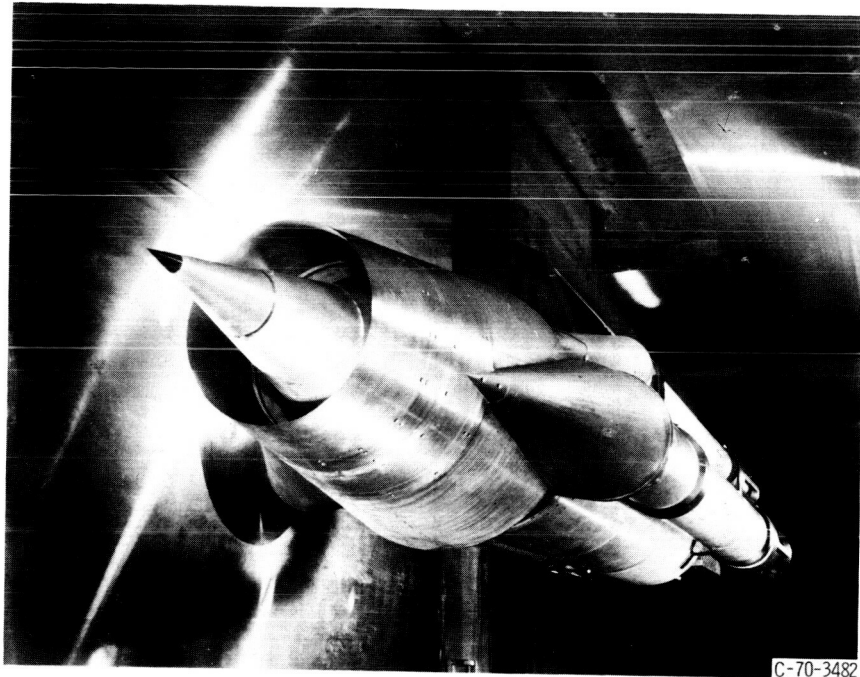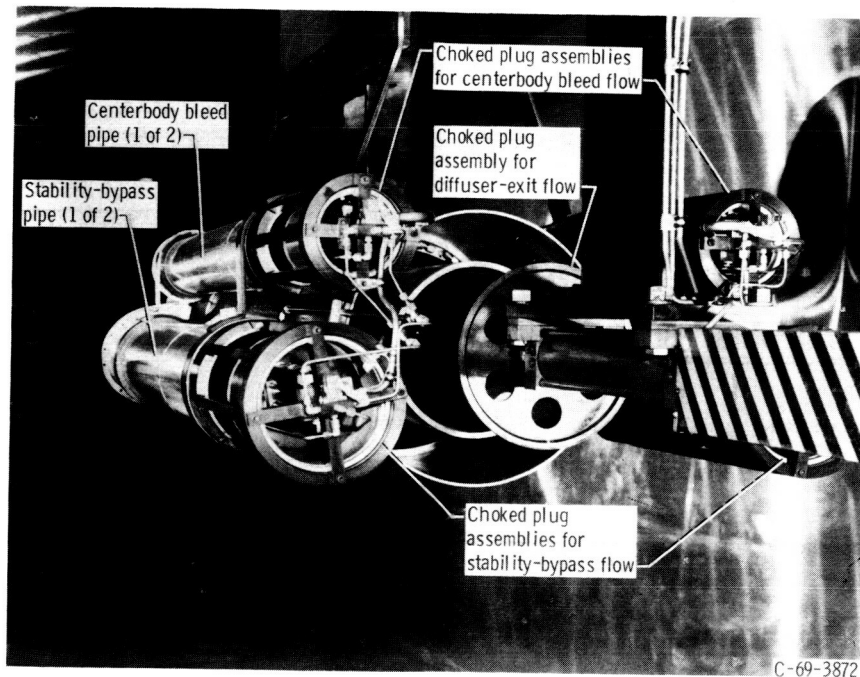
(b) Rear view.

Figure 1. - Model installed in wind tunnel.

28

Cowl surface conditions

Inlet contour

Axial distance from cone tip, x/R_c, inlet radii

Centerbody surface conditions
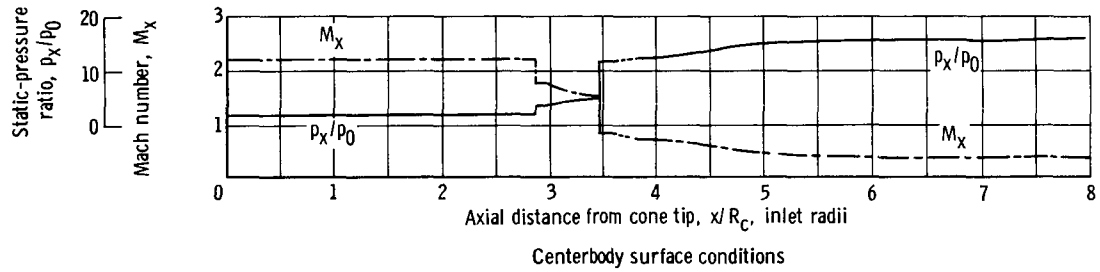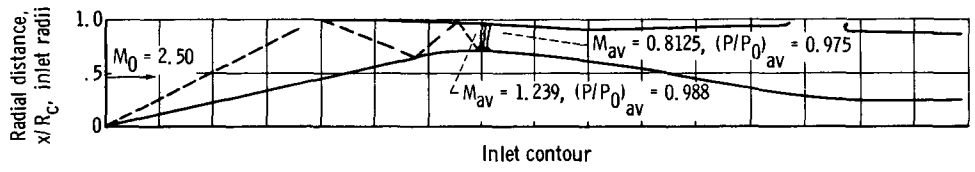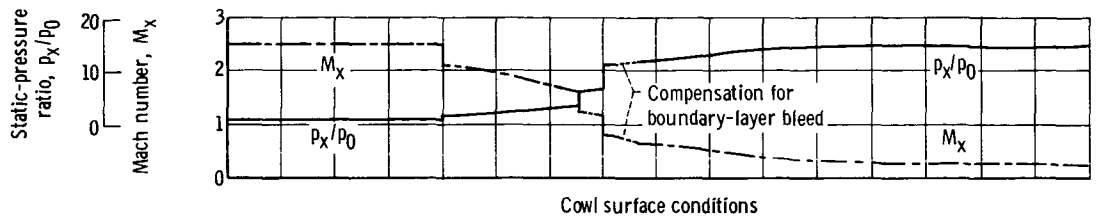
(a) Inlet dimensions and theoretical flow conditions.

Axial distance from cone tip, x/R_c, inlet radii
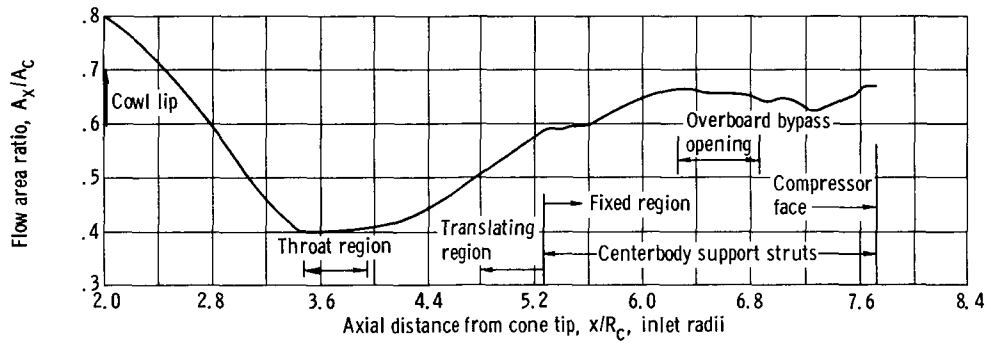
(b) Diffuser area variation for $\theta_l = 26.72°$.

Figure 2. - Aerodynamic details.

93.70
3.960

182.55
7.716

174.98
7.396

Fast acting overboard bypass
Overboard bypass entrance
Large stability-bypass plenum
Poppet valves
Small stability-bypass plenum
Stability-bypass entrance

Stability-bypass pipe

Stability-
bypass
airflow

Ejector
bypass

Dual-vane
cascade

Choke plate
position

$R_c = 23.66$

12.5°

Forward cowl
bleed region

Centerbody
bleed region

Vortex generators

Strut discharge louvers

Centerbody
bleed airflow

Centerbody bleed pipe

CD-11600-01

Figure 3. – Inlet details. (All linear dimensions are in cm.)

Diffuser-exit total-
pressure rakes

Cowl

C D C D C D C
D   D

Centerline of
centerbody
support struts

Looking downstream. (C denotes converging pair; D denotes diverging pair.)

Upper surface coordinates
from NACA 0012 airfoil
(lower surface is flat)

Leading edge,
0.0254 rad

0.1524

2.54

1.27

Flow

16°

3.95   3.95
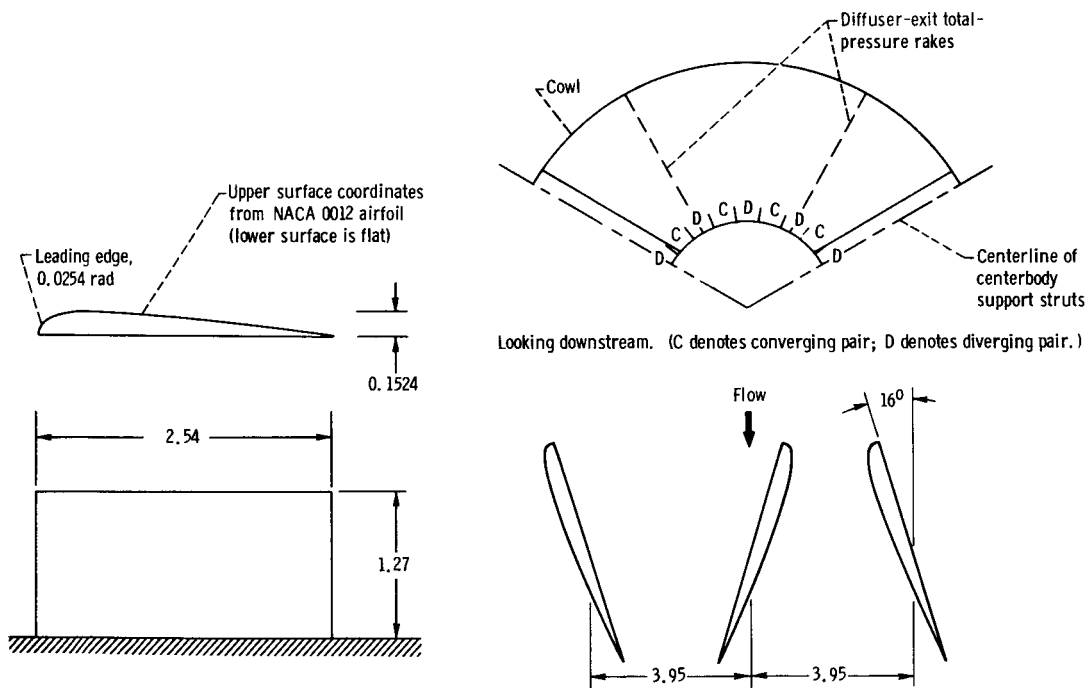
Figure 4. – Vortex generator design. (All linear dimensions are in cm.)
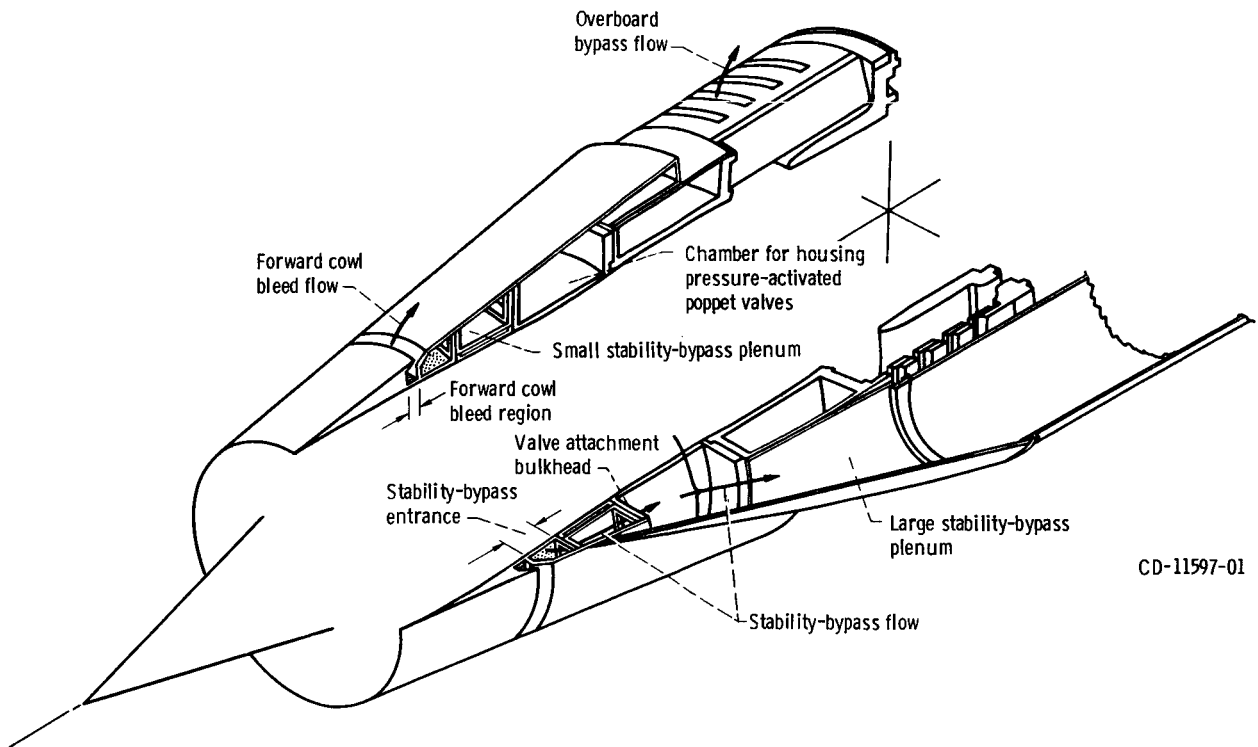
Figure 5. - Sketch of inlet cowl showing cowl bleed and bypass ducting.

CD-11597-01

Overboard
bypass flow

Chamber for housing
pressure-activated
poppet valves

Forward cowl
bleed flow

Small stability-bypass plenum

Forward cowl
bleed region

Valve attachment
bulkhead

Stability-bypass
entrance

Large stability-bypass
plenum
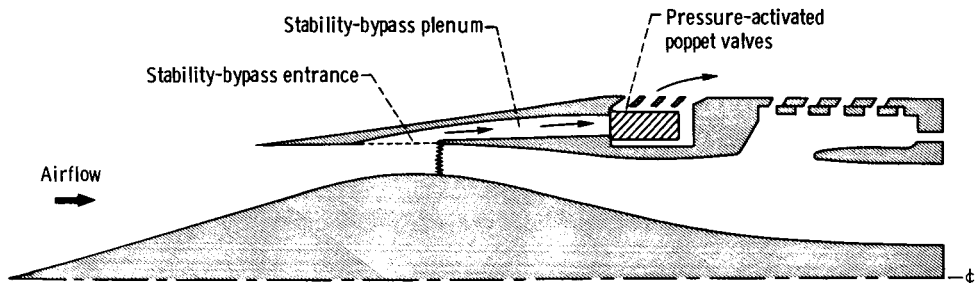
Stability-bypass flow

Figure 6. - Possible arrangement of a stability-bypass system for a flight inlet.

CD-11412-01

Stability-bypass plenum

Pressure-activated
poppet valves

Stability-bypass entrance

Airflow

Hole pattern

Exit area = 89.56 cm^2

Small stability-
bypass plenum

Geometric
throat

Axial distance, x/R_c, inlet radii 3.160 3.247

3.282   3.496 3.579

Forward cowl bleed region;
6 rows of 40 percent porosity
normal porous bleed

Stability bypass entrance;
18 rows of 40 percent porosity
normal porous bleed

(a) Distributed porous stability-bypass entrance. Hole diameter, 0.3175 centimeter.

Hole pattern
Exit area = 89.56 cm^2

Small slot insert

Small stability-
bypass plenum

0.725

1.452

20°

3.314

0.152 rad.

Axial distance, x/R_c, inlet radii 3.160 3.265   3.405 3.496

Geometric
throat

Forward cowl bleed region;
7 rows of 40 percent porosity
normal porous bleed

Stability-
bypass
entrance

(b) Forward-slanted slot stability-bypass entrance.

0.318

10°

Exit area = 89.56 cm^2

Small stability-
bypass plenum

0.114

1.270

Typical slot

Axial distance,
x/R_c, inlet radii 3.156 3.264   3.496 3.545

Geometric
throat

Forward cowl
bleed region

Stability-
bypass entrance

(c) Distributed educated stability-bypass entrance.

Figure 7. – Forward cowl bleed and stability-bypass entrance arrangements.
(Dimensions are in cm unless otherwise noted.)

Theoretical shock pattern

Air flow

Experimental shock pattern

Geometric throat

Distributed porous

Small slot insert

Large or small forward slanted slot

Distributed educated

Figure 9. – Inlet stability-bypass entrance and bleed region configurations.

Bypass entrance type	Forward cowl bleed region	Stability-bypass entrance	Centerbody bleed region
Distributed porous	■■■■□□	■■■■■■□□□□□□□□□	□□□□□□■■
Large or small forward-slanted slot	■■■■□□□	(slot)	□□□□□□■■
Distributed educated	▽▼	▽▽▽▽▽	□□□□□□■■

□ Hole row open ▽ Educated slot open
■ Hole row closed ▼ Educated slot closed

Airflow

Axial distance, x/R_c, inlet radii: 3.315 3.385 3.475
Geometric throat

3.349 | 3.419
3.332 | 3.402
3.367 3.438
3.504
3.553
3.602
3.702
3.800

Figure 8. – Centerbody bleed arrangement. Hole diameter, 0.3175 centimeter.

33

(a) Poppet valve installation, several valve positions shown.
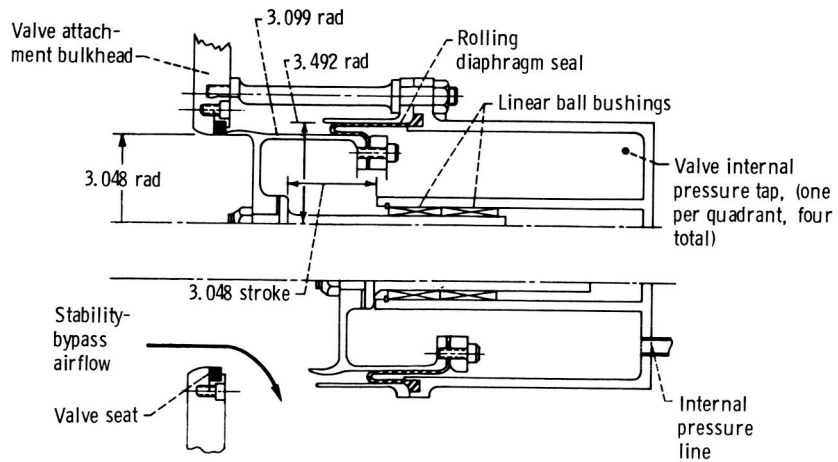
(b) Poppet-valve details. Dimensions are in centimeters.

Figure 10. - Poppet valve.

Simulated
stability-bypass
total pressure,
P_{sb}

Valve
attachment
bulkhead

Valve chamber

Exhaust pressure, p_e

Mass
flow,
m_{pv}

Supply
flow

Poppet valve
(internal
pressure, p_{pvi})

To
exhaust

$\dfrac{P_{sb}}{p_e} > 2$

Schematic of bench test

Valve operating pressure, $P_{sb}/P_{sb,ref}$

○ Flow choked at valve opening
● Flow choked at bulkhead opening

1.4

1.2

1.0

.8

0   .2   .4   .6   .8   1.0

Valve mass-flow ratio, $m_{pv}/m_{pv,ref}$

(c) Poppet-valve performance. Initial stability-bypass
total pressure, P_{sb} = 3.1 N/cm^2; reference pressure,
$P_{sb,ref}$ = 3.9 N/cm^2; exhaust pressure, p_e = 0.77 to
1.01 N/cm^2.

Figure 10. - Concluded.

35

Downstream view

○ Total-pressure probe
● Static-pressure tap

Rake 5, 332.5°
Rake 6, 27.5°
Strut centerline
Rake 4, 267.5°
Rake 1, 92.5°
Rake 3, 212.5°
Rake 2, 147.5°
Hollow centerbody support struts

Cowl   d/H
0.982
.945
.907
.829
.699
H = 14.905 cm   .552
.378
.236
d   .151
.047
Centerbody
Typical diffuser exit
rake; x/R_c = 7.396
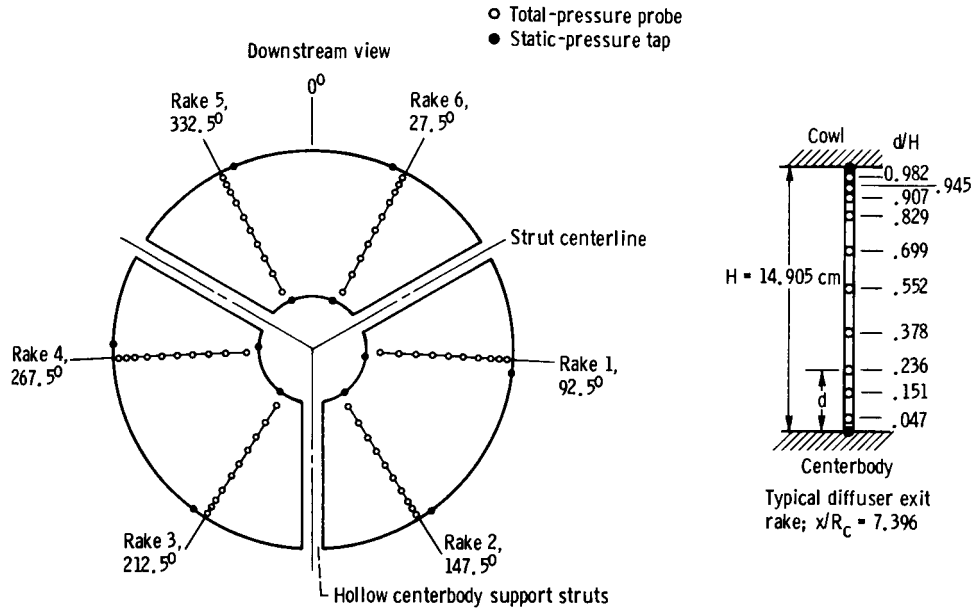
(b) Total- and static-pressure instrumentation at diffuser-exit station, x/R_c = 7.396.

Total
Static
Forward cowl
pressure probes
Stability-bypass
total-pressure rakes
φ = 90°, 270°
Axial distance,
x/R_c, 4.086
Overboard bypass plenum
total-pressure probe
Centerbody base
total-pressure probe
CD-11611-01
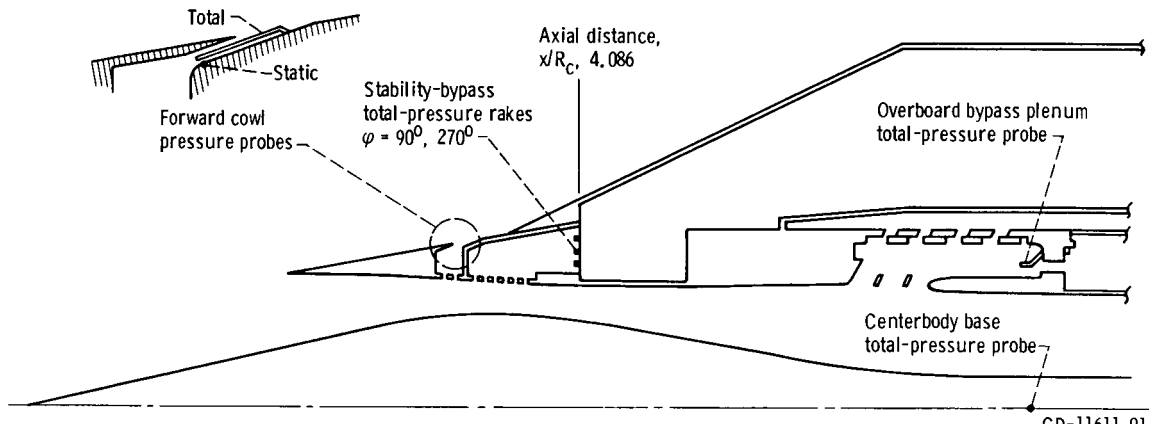
(c) Bleed and bypass pressure instrumentation.

Figure 11. - Inlet-pressure instrumentation (x/R_c is the axial distance from cone tip, φ is the circumferential position, and d/H is the ratio of distance from surface to annulus height).

36
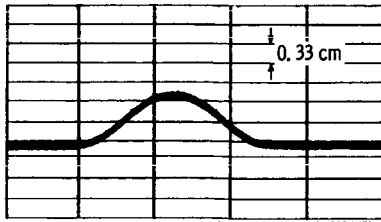
(a) Commanded overboard-bypass-door move-
ment.

-.01　　0　　.01　　.02　　.03　　.04
Time measured from start of transient, sec
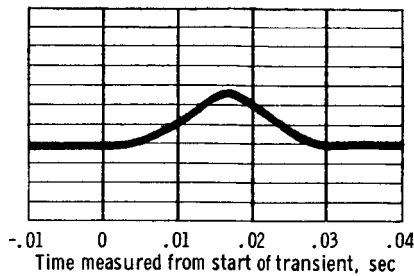
(b) Overboard-bypass-door response.

Figure 12. - Overboard-bypass-door response
at a transient pulse frequency of 40 sec⁻¹.
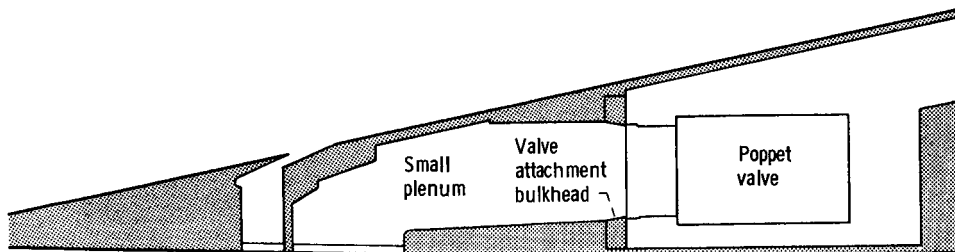
(a) Poppet valves closed; small stability-bypass plenum volume.
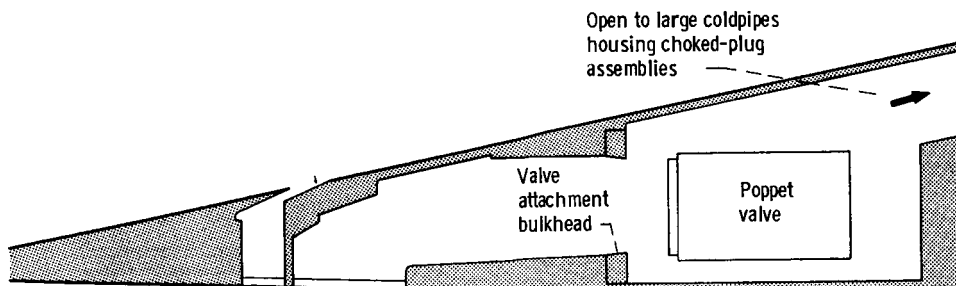
(b) Poppet valves open; large stability-bypass plenum volume.

Figure 13. - Small and large stability-bypass plenum volumes.
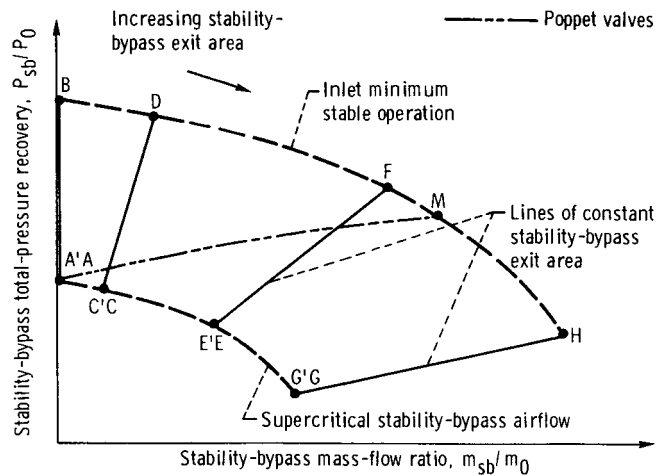
(a) Stability bypass performance.
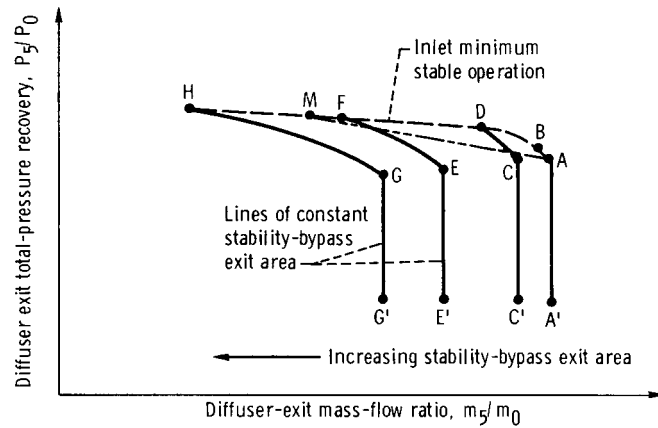
(b) Inlet performance.
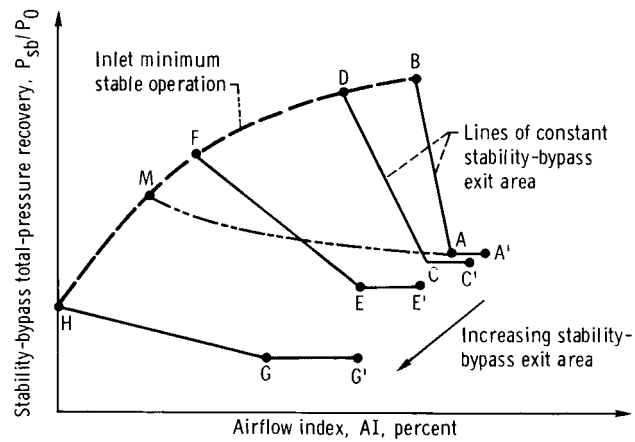
(c) Airflow index.

Figure 14. – Stylized inlet stability data.

Stability-bypass entrance configuration	Total-pressure recovery		Mass-flow ratio	
	P_5/P_0	P_{sb}/P_0	m_{fc}/m_0	m_{cb}/m_0
Distributed porous	0.887	0.426	0.016	0.021
Large forward-slanted slot	.873	.556	.019	.032
Small forward-slanted slot	.893	.497	.019	.022
Distributed educated	.885	.426	.008	.022
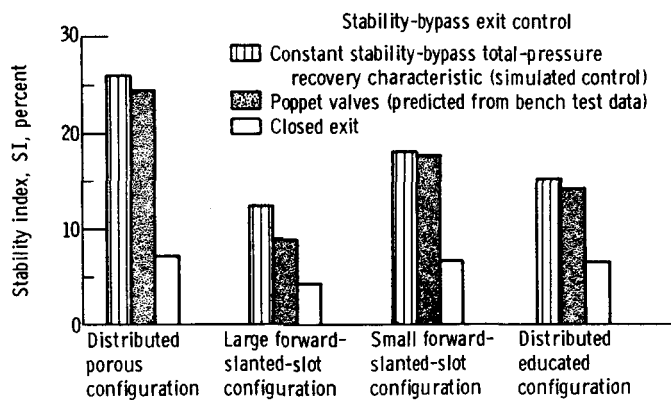
Figure 15. - Stability index obtained with various stability-bypass exit controls and stability-bypass entrance configurations. Stability-bypass mass-flow ratio at inlet operating points, m_{sb}/m_0, 0. (See table for other inlet-operating-point conditions.)
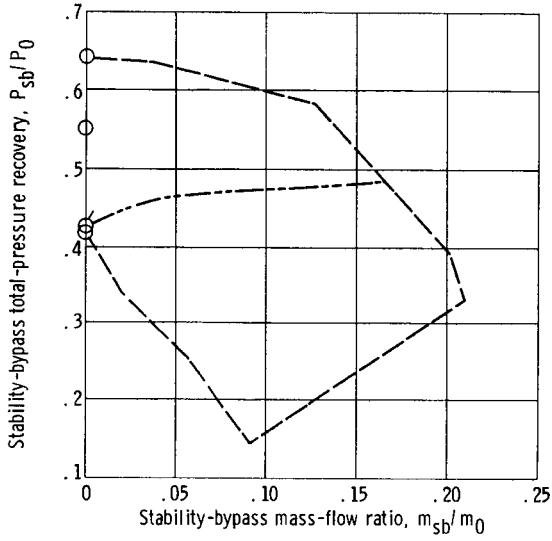
(a) Stability-bypass performance.
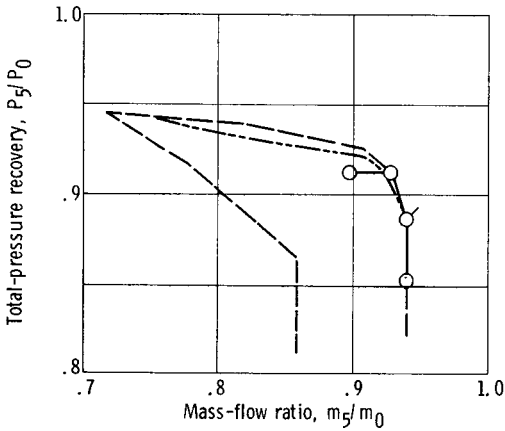
(b) Inlet performance.

(c) Airflow index.

Stability-bypass exit control

○   Closed exit
—·—·—   Poppet valves (predicted from bench test data)
— — —   Performance envelope (distributed porous configuration of ref. 8)

Tailed symbol denotes inlet operating point
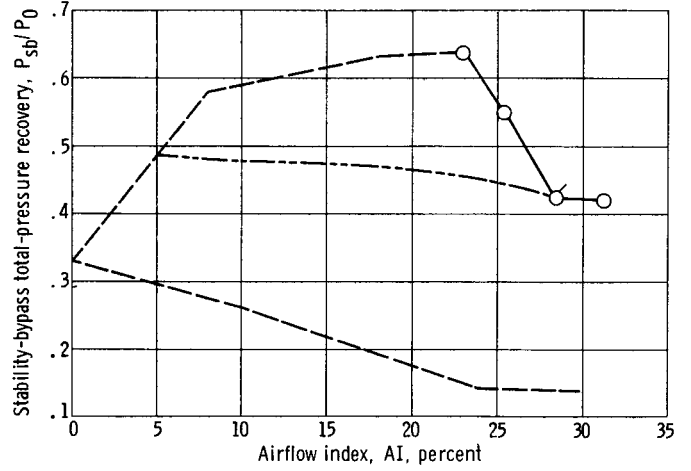
Figure 16. – Performance of stability-bypass exit controls with distributed porous stability-bypass entrance configuration.
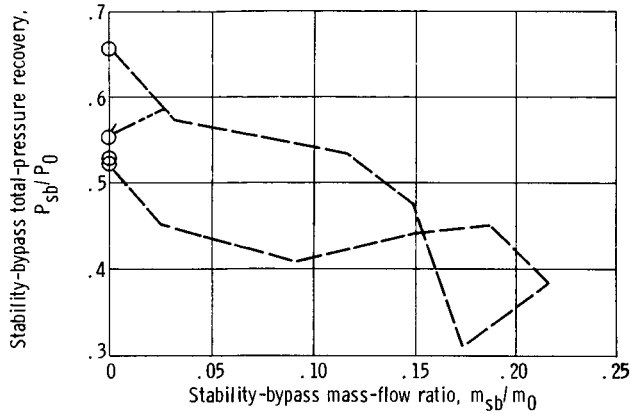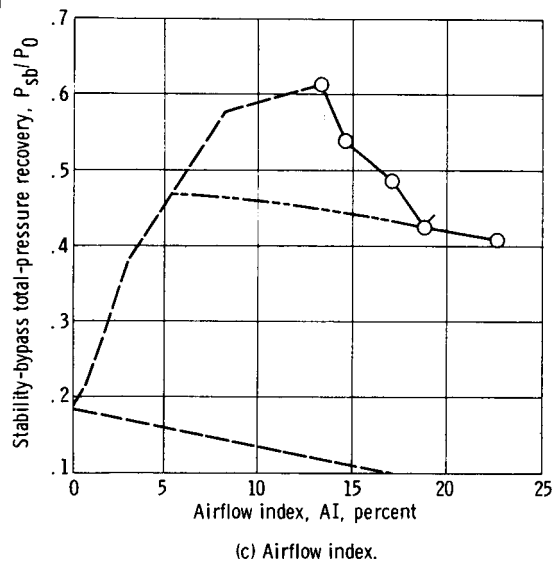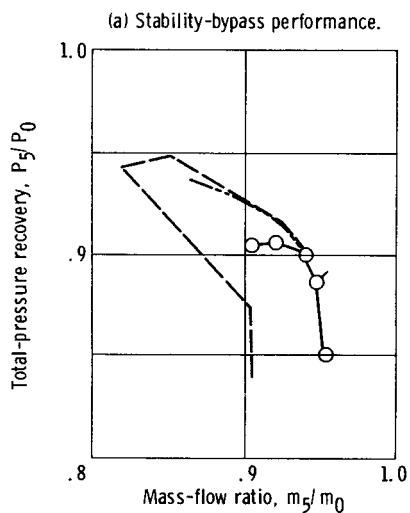
Figure 17. – Performance of stability-bypass exit controls with large forward-slanted-slot stability-bypass entrance configuration.
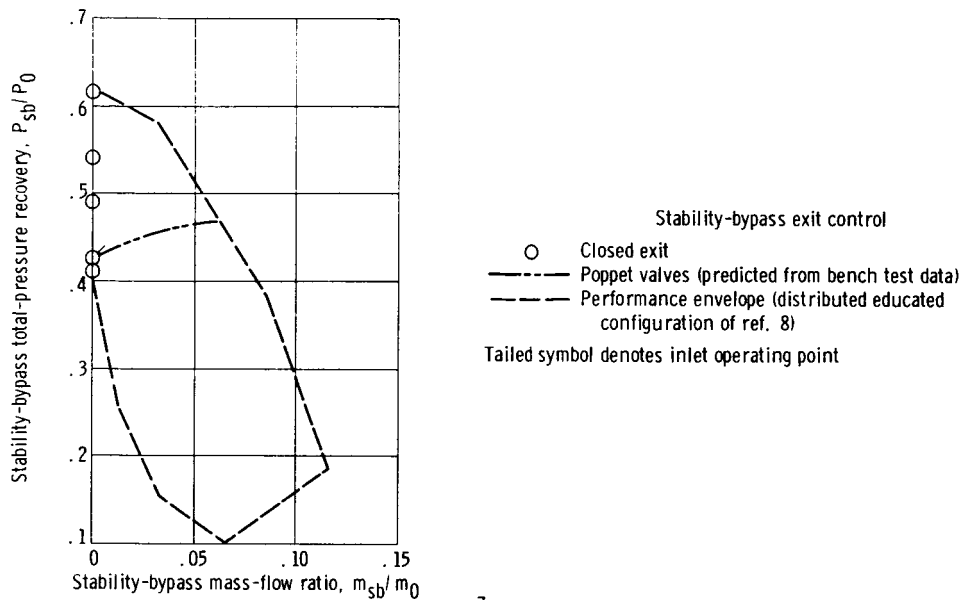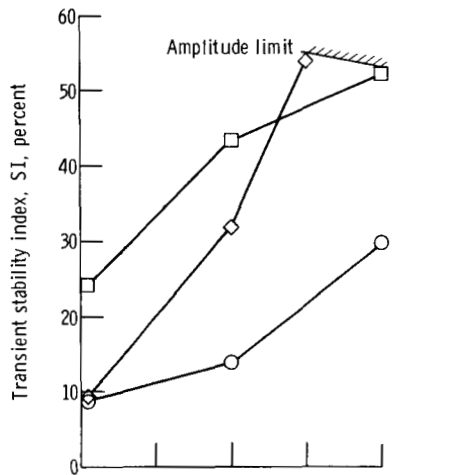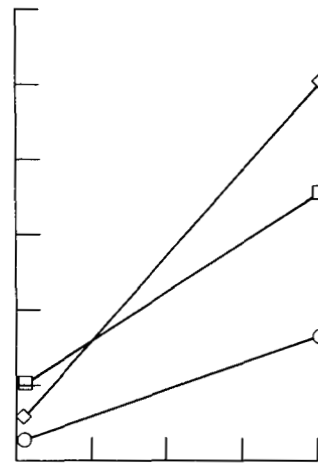
Stability-bypass exit control

○   Closed exit

— · — · —   Poppet valves (predicted from bench test data)

— — — —   Performance envelope (small forward-slanted-slot configuration of ref. 8)

Tailed symbol denotes inlet operating point

(a) Stability-bypass performance.

(b) Inlet performance.

(c) Airflow index.

Figure 18. – Performance of stability-bypass exit controls with small forward-slanted-slot stability-bypass entrance configuration.

(a) Stability-bypass performance.

(b) Inlet performance.

(c) Airflow index.

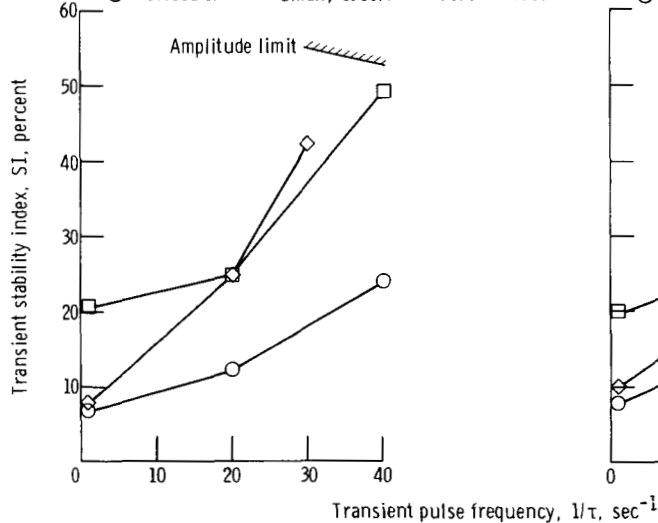Figure 19. – Performance of stability-bypass exit controls with distributed educated stability-bypass entrance configuration.

	Stability-bypass exit control	Stability-bypass plenum volume, m^3	Total-pressure recovery, P_5/P_0	P_{sb}/P_0
□	Poppet valves	Small, 0.0175	0.876	0.417
◇	Closed exit	Large, 0.398	.877	.424
○	Closed exit	Small, 0.0175	.874	.432

(a) Distributed porous stability-bypass entrance configuration.

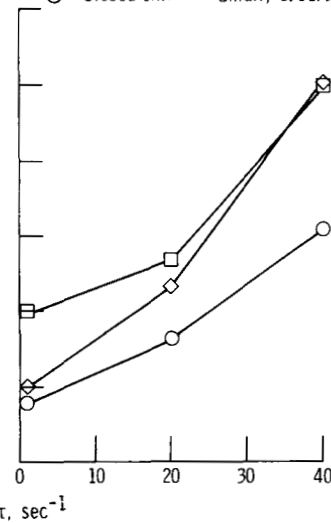|	Stability-bypass exit control	Stability-bypass plenum volume, m^3	Total-pressure recovery, P_5/P_0	P_{sb}/P_0
□	Poppet valves	Small, 0.0096	0.866	0.585
◇	Closed exit	Large, 0.390	.880	.542
○	Closed exit	Small, 0.0096	.868	.590

(b) Large forward-slanted-slot stability-bypass entrance configuration.

	Stability-bypass exit control	Stability-bypass plenum volume, m^3	Total-pressure recovery, P_5/P_0	P_{sb}/P_0
□	Poppet valves	Small, 0.0073	0.876	0.498
◇	Closed exit	Large, 0.388	.878	.498
○	Closed exit	Small, 0.0073	.878	.509

(c) Small forward-slanted-slot stability-bypass entrance configuration.

	Stability-bypass exit control	Stability-bypass plenum volume, m^3	Total-pressure recovery, P_5/P_0	P_{sb}/P_0
□	Poppet valves	Small, 0.0175	0.878	0.421
◇	Closed exit	Large, 0.398	.877	.423
○	Closed exit	Small, 0.0175	.878	.432

(d) Distributed educated stability-bypass entrance configuration.

Figure 20. – Unstart limits of inlet-coldpipe combination using stability-bypass system when subjected to transient disturbances.
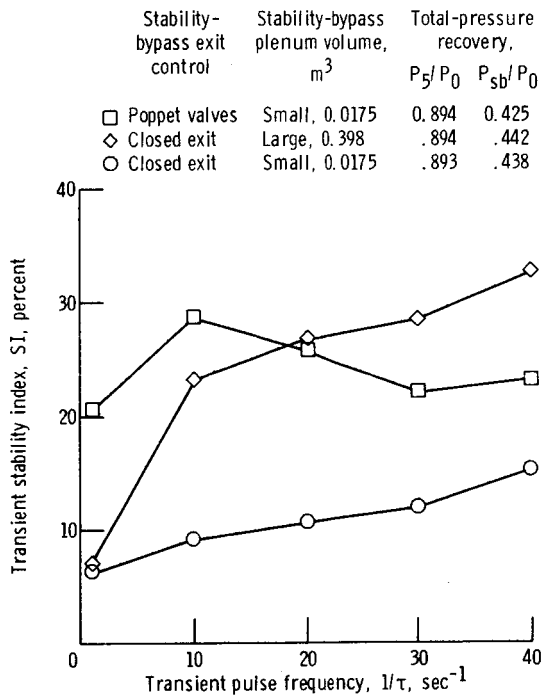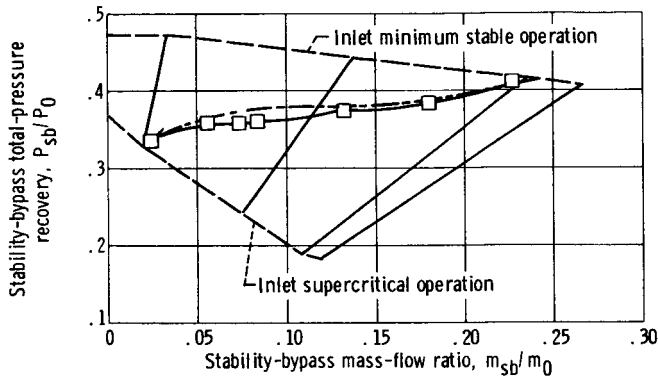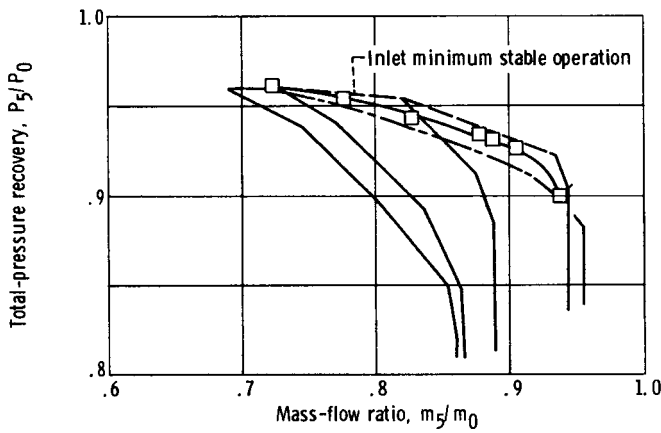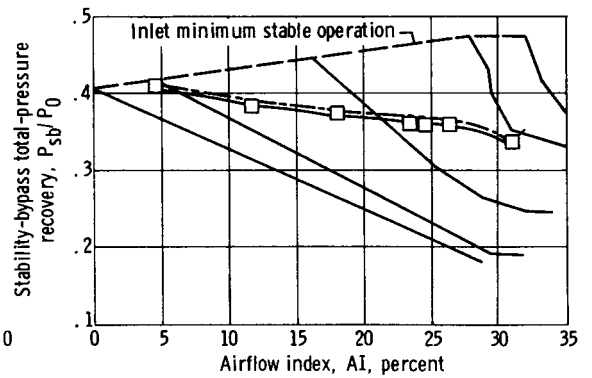
Stability- bypass exit control	Stability-bypass plenum volume, m^3	Total-pressure recovery,	
		P_5/P_0	P_{sb}/P_0
□ Poppet valves	Small, 0.0175	0.894	0.425
◇ Closed exit	Large, 0.398	.894	.442
○ Closed exit	Small, 0.0175	.893	.438

Figure 21. – Unstart limits of inlet with choke plate and distributed porous stability-bypass entrance configuration when subjected to transient disturbances.

Figure 22. – Comparison of predicted and experimental poppet valve performance using stability-bypass system installed in alternate inlet (distributed-porous configuration II of ref. 4).

46